

## Well-Defined Silica-Supported Calcium Reagents: Control of Schlenk Equilibrium by Grafting

Régis M. Gauvin,<sup>\*[a]</sup> Frank Buch,<sup>[b]</sup> Laurent Delevoye,<sup>[a]</sup> and Sjoerd Harder<sup>\*[b]</sup>

**Abstract:** Calcium reagents  $\text{Ca}(\alpha\text{-Me}_3\text{Si-2-Me}_2\text{N-benzyl})_2 \cdot 2 \text{ thf}$  (**1**) and  $\text{Ca}[\text{N}(\text{SiMe}_3)_2]_2 \cdot 2 \text{ thf}$  (**2**) reacted with silica partially dehydroxylated at 700 °C to afford materials that bear  $(\equiv \text{SiO})\text{Ca}(\alpha\text{-Me}_3\text{Si-2-Me}_2\text{N-benzyl}) \cdot 1.6 \text{ thf}$  (**SiO<sub>2</sub>-1**) and  $(\equiv \text{SiO})\text{Ca}[\text{N}(\text{SiMe}_3)_2] \cdot 1.3 \text{ thf}$  (**SiO<sub>2</sub>-2**) fragments, respectively. Due to the bulk of the supported complexes, the silanol groups are only partially metalated: 50% in **SiO<sub>2</sub>-1** and 70% in **SiO<sub>2</sub>-2**. In the case of **SiO<sub>2</sub>-2**, a parallel  $\text{SiMe}_3$ -capping side reaction affords in fine a silanol-free surface. The materials were characterized by IR spectroscopy, 1D and 2D solid-state high-field NMR spectroscopy,

and elemental analysis. Reaction of **2** with one equivalent of the bulky silanol ( $t\text{BuO}$ )<sub>3</sub>SiOH, a silica-surface mimic, afforded the homoleptic bis-silyloxy calcium derivative through ligand exchange (Schlenk equilibrium), and a derivative was isolated and structurally characterized. Preliminary studies have shown that both grafted benzyl and amide derivatives are active in olefin hydrosilylation, intramolecular hydroamination, and styrene polymeri-

zation, with evidence showing that catalysis occurs through supported species. In styrene polymerization, a marked influence of the surface acting as a ligand on the stereoselectivity of the reaction was observed, as syndiotactic-rich polystyrene (88% of *r* diads) was obtained. These results illustrate that grafting of calcium benzyl or amide compounds on a silica surface is a new concept to prevent ligand exchange through the Schlenk equilibrium. Heteroleptic calcium complexes that cannot be synthesized as stable molecular species in solution can be obtained as silica-supported species which have been shown to be catalytically active.

**Keywords:** calcium • heterogeneous catalysis • silica • supported catalysts • surface chemistry

### Introduction

Heterogenization of a catalyst is generally applied in the development of cleaner processes based on recyclable materials. Although this is one of the most interesting aspects of catalyst immobilization, it is equally important to note that the chemistry of a catalyst can be significantly altered by its anchoring onto a support.<sup>[1]</sup> Indeed, grafting may block multimolecular deactivation processes or prevent aggregation of

intermediate reactive centers into inactive species. Even if, from a simplified molecular point of view, the silica surface may be considered as a bulky alkoxide, it still differs from soluble models<sup>[2]</sup> or bulky ligands<sup>[3]</sup> in two ways: 1) the latter often bury the metal center within a pocket that makes it unreactive or less reactive and 2) molecular model ligands may sterically and electronically mimic the silica surface but do not take into account the enforced immobility of silica-supported species. Distinct chemistry may thus be expected from grafted systems.

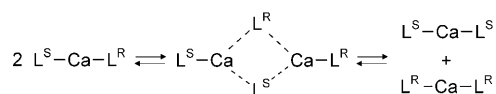
Here we present the first studies on grafting of calcium reagents on a silica surface. Our interest in grafted calcium species stems from the rapidly growing application of calcium reagents as green catalysts.<sup>[4]</sup> As calcium is one of the cheapest and most accessible metals worldwide, we are not interested in recycling a potential calcium catalyst, but our motivations are based on two practical aspects. First, instead of application in a batch process grafted catalysts can be advantageously used in continuous processes. Second, organocalcium chemistry is often plagued by the Schlenk equilibrium that is well-known for Grignard reagents.<sup>[5]</sup> Calcium catalysts in general are composed of an inactive spectator

[a] Dr. R. M. Gauvin, Dr. L. Delevoye  
Unité de Catalyse et de Chimie du Solide UMR CNRS 8181  
Ecole Nationale Supérieure de Chimie  
BP 90108, 59652 Villeneuve d'Ascq Cedex (France)  
Fax: (+33) 320-43-67-54  
E-mail: regis.gauvin@ensc-lille.fr

[b] F. Buch, Prof. Dr. S. Harder  
Anorganische Chemie, Universität Duisburg-Essen  
Universitätsstrasse 5, 45117 Essen (Germany)  
Fax: (+49) 201-183-2621  
E-mail: sjoerd.harder@uni-due.de

Supporting information for this article is available on the WWW under <http://dx.doi.org/10.1002/chem.200802512>.

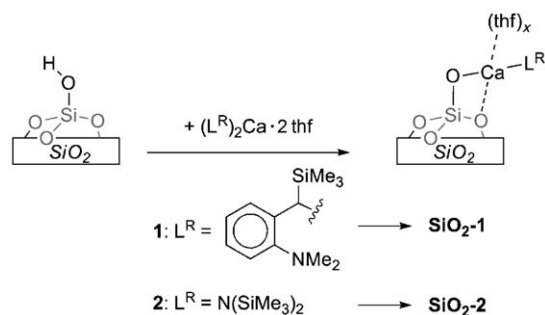
ligand ( $L^S$ ) and a reactive ligand ( $L^R$ ), responsible for catalyst activity. A Schlenk equilibrium between heteroleptic and homoleptic complexes would result in an undefined mixture of potential catalytically active species (Scheme 1).



Scheme 1. Schlenk equilibrium via an associative transition state;  $L^R$  and  $L^S$  represent reactive and spectator ligands, respectively.

As ligand exchange likely proceeds through a bimolecular associative process, immobilization of the calcium reagent could prevent such Schlenk equilibria. In addition, a solid support can also be used to prevent aggregation of calcium reagents. Thus, distinct highly reactive mononuclear calcium sites may be obtained.

The complexes  $\text{Ca}(\text{DMAT})_2 \cdot 2\text{thf}$  (**1**;  $\text{DMAT} = \alpha\text{-Me}_3\text{Si-}o\text{-Me}_2\text{N-benzyl}$ )<sup>[6]</sup> and  $\text{Ca}[\text{N}(\text{SiMe}_3)_2]_2 \cdot 2\text{thf}$  (**2**)<sup>[7]</sup> are versatile reactive precursors in calcium chemistry<sup>[6]</sup> and show catalytic activity in various reactions.<sup>[4]</sup> Therefore, we targeted these reagents for immobilization on a silica surface.<sup>[8]</sup> As calcium is divalent we must selectively prepare sites comprising a single calcium-to-surface bond. This should leave a catalytically active bond or at least a reactive functionality amenable to activation. In this regard, the support of choice appears to be Aerosil 380 that has been dehydroxylated at 700 °C under a secondary vacuum. This type of nonporous silica, which we designate here as  $\text{SiO}_2\text{-700}$ , bears isolated silanol groups as the sole type of protic site, a prerequisite for synthesis of the targeted single-site catalysts.<sup>[9]</sup> In addition, the high reactivity of complexes **1** and **2** towards the acidic silanol groups in  $\text{SiO}_2\text{-700}$  warrants efficient grafting. Considering that the density of silanol groups is about  $1.1 \text{ nm}^{-2}$ ,<sup>[10]</sup> which translates to an average spacing of 11 Å, treatment of  $\text{SiO}_2\text{-700}$  with a solution of **1** or **2** would merely give isolated heteroleptic calcium benzyl or amide groups (Scheme 2). Furthermore, the lack of porosity of the Aerosil support will avoid dependence of the catalytic performance on diffusion of reagents and products to and from surface active sites.



Scheme 2. Preparation of  $\text{SiO}_2\text{-1}$  and  $\text{SiO}_2\text{-2}$ .

We report here experimental procedures for grafting of calcium reagents and extensive analyses of the immobilized species (elemental analyses, IR spectroscopy, and various state-of-the-art solid-state NMR techniques). In addition, we describe preliminary studies on the use of grafted calcium catalysts in alkene hydrosilylation, intramolecular alkene hydroamination, and polymerization of styrene.

## Results and Discussion

**Reaction of  $\text{Ca}(\text{DMAT})_2 \cdot 2\text{thf}$  (**1**) with  $\text{SiO}_2\text{-700}$ : synthesis and characterization of  $\text{SiO}_2\text{-1}$ :** Overnight stirring of a yellow toluene solution of  $\text{Ca}(\text{DMAT})_2 \cdot 2\text{thf}$  (**1**) with  $\text{SiO}_2\text{-700}$  affords, after washing with toluene, a yellow material ( $\text{SiO}_2\text{-1}$ ), the color of which fades on exposure to air (Scheme 2). Elemental analysis indicates a Ca loading of 1.26 wt %, which corresponds to 0.55 Ca per square nanometer. As the initial silanol concentration is  $1.1 \text{ nm}^{-2}$ , half of the silanol groups reacted with the molecular precursor to afford the grafted species. The origin of incomplete consumption of silanol groups could be the bulk of the supported  $\text{Ca}(\text{DMAT})_x \cdot \text{thf}$  fragment. This hinders approach of the molecular precursor and thus prevents reaction of residual silanol groups.<sup>[11]</sup> The contents of nitrogen (0.50 wt %) and carbon (8.01 wt %) indicate N/Ca and C/N ratios of 1.15 and 18.51, respectively. This is consistent with the formation of  $(\equiv\text{SiO})\text{Ca}(\text{DMAT}) \cdot 1.6\text{thf}$  surface species. Such a stoichiometry indicates that the silica surface, which can be regarded as a ligand, is slightly bulkier than the bidentate DMAT ligand (in comparison: **1** bears two THF ligands per Ca atom).

We also monitored DMAT-H formation during the grafting process by  $^1\text{H}$  NMR spectroscopy on a mixture of  $\text{Ca}(\text{DMAT})_2 \cdot 2\text{thf}$  (**1**) and  $\text{SiO}_2\text{-700}$  in  $\text{C}_6\text{D}_6$ . As the concentration of DMAT-H does not increase after measurement of the first spectrum (10 min) the reaction of the benzyl calcium complex with the silica support is fast. Quantification of catalyst loading by using ferrocene as an internal standard gives a Ca content of 1.29 wt %, a value close to that obtained from elemental analysis (1.26 wt %). This confirms that protonolysis of the calcium-carbon bond is indeed the main reaction and that the proposed stoichiometry is correct.

This protonolysis reaction was also confirmed by infrared studies on  $\text{SiO}_2\text{-1}$  (Figure 1). The IR spectrum of  $\text{SiO}_2\text{-700}$  shows a typical sharp isolated silanol signal at  $3747 \text{ cm}^{-1}$ , which is not observed in IR spectra of  $\text{SiO}_2\text{-1}$ . Instead, a broad, low-intensity signal centered at  $3620 \text{ cm}^{-1}$  indicates the presence of residual silanol groups, as already deduced from the measured calcium loading. The broadness of this peak is most probably due to interaction with neighboring grafted species.<sup>[11]</sup> The  $\nu(\text{sp}^2 \text{ C-H})$  and  $\nu(\text{sp}^3 \text{ C-H})$  peaks in the  $3097\text{--}3020 \text{ cm}^{-1}$  and  $2981\text{--}2785 \text{ cm}^{-1}$  regions, respectively, of the spectrum of  $\text{SiO}_2\text{-1}$  are similar to those of the molecular precursor, as are the peaks related to aromatic rings in the  $1600 \text{ cm}^{-1}$  and  $1490\text{--}1450 \text{ cm}^{-1}$  regions.<sup>[12]</sup>

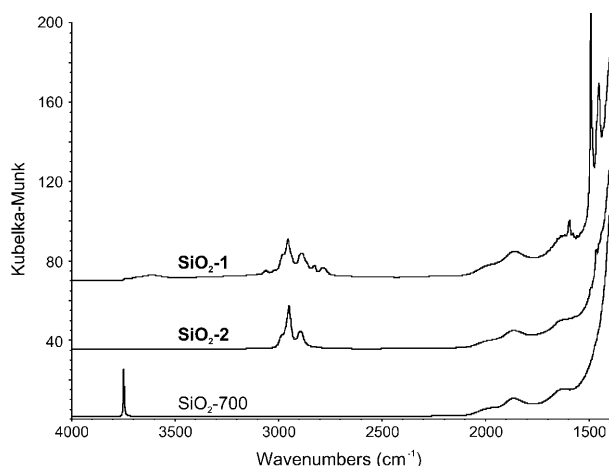


Figure 1. DRIFT spectra of SiO<sub>2</sub>-700, SiO<sub>2</sub>-2, and SiO<sub>2</sub>-1.

In addition, SiO<sub>2</sub>-1 was investigated by high-field state-of-the-art solid-state NMR spectroscopy. This is a powerful technique to obtain information on a material at the molecular level. It provides information on the environment of observed nuclei through their chemical shifts and also from correlation between the different sites.

Solid-state NMR spectra were recorded on an 18.8 T spectrometer (800.13 MHz <sup>1</sup>H frequency). Figure 2a presents the <sup>1</sup>H MAS NMR spectrum of SiO<sub>2</sub>-1. It has several

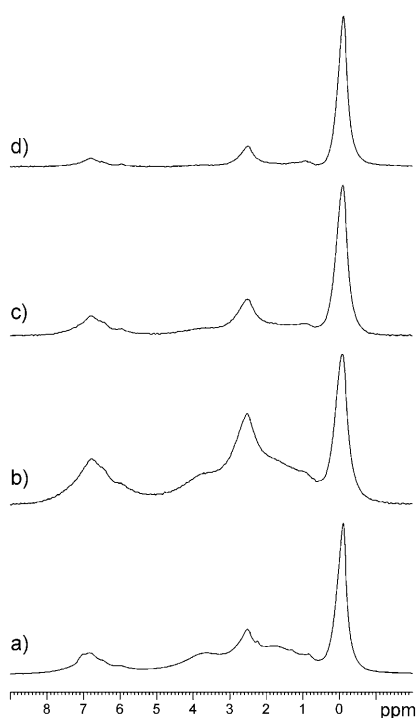


Figure 2. <sup>1</sup>H MAS NMR spectra of SiO<sub>2</sub>-1 acquired using a) a single-pulse sequence, b) an excitation/reconversion pulse train of one rotor period, c) two rotor periods, and d) four rotor periods (800.13 MHz, 20 kHz spinning speed, 64 transients except for a), for which 16 transients were recorded). The excitation/reconversion trains were composed of back-to-back pulses of 2.1 μs).

features characteristic of the expected grafted species: a sharp peak at  $\delta=0.0$  ppm for the Me<sub>3</sub>Si group, signals at  $\delta=6.8$ – $6.0$  ppm for the aromatic protons, a signal at  $\delta=2.6$  ppm originating from the Me<sub>2</sub>N groups, and a broad distribution between  $\delta=4$  and  $0.5$  ppm that could be assigned to the THF ligand(s) and to the methyne proton. The grafted species contains both rigid (DMAT) and mobile (THF) moieties for which the relaxation behavior is expected to vary considerably. Therefore, it may be possible to filter the signals in order to selectively observe a fragment. <sup>1</sup>H–<sup>1</sup>H double-quantum MAS spectroscopy (DQ-MAS) provides information about the spatial proximity of protons by means of dipolar recoupling pulse sequences. In the BABA (back to back) sequence,<sup>[13]</sup> for example, rotor-synchronized pulses are used to create double-quantum coherence and, after a t1 evolution period for 2D acquisition, convert them to single-quantum coherences. The BABA sequence can also be used to filter out the signals of mobile protons from those in a rigid configuration. Indeed, the correlation information obtained by increasing the number of rotor cycles is in direct competition with the simultaneous relaxation phenomenon, which occurs during pulse excitation and reconversion. Applying four rotor cycles for excitation and reconversion periods to SiO<sub>2</sub>-1 affords a spectrum in which the THF proton signals are of considerably lower intensity, and thus the spectrum of the DMAT ligand alone is revealed. The filtered spectrum allows for detection of the rather weak benzylic methyne proton signal at  $\delta=0.9$  ppm. (Figure 2d). The assignment of the ArCHSiMe<sub>3</sub> proton signal is consistent with the corresponding <sup>1</sup>H NMR data of the molecular precursor **1** in solution ( $\delta=0.9$  and 1.24 ppm). An intermediate situation is observed for spectra recorded with the sequence synchronized with one and two rotor cycles (Figure 2b and c, respectively).

The spatial proximities between the protons of SiO<sub>2</sub>-1 can be assessed by using double-quantum correlation spectroscopy. Use of the back-to-back train pulse synchronized with four rotor cycles affords a correlation map comprising several off-diagonal signals (Figure 3).

Two pairs associate the aromatic signals around  $\delta=6.8$  ppm with the  $\delta=0.0$  ppm and  $\delta=2.6$  ppm peaks (Figure 3, top left: interactions A and B, respectively). The third off-diagonal correlation involves the signals at  $\delta=2.6$  and  $0.0$  ppm (interaction C). The observed proximity between aromatic signals and the Me<sub>3</sub>Si or Me<sub>2</sub>N protons is in agreement with the structure of the proposed surface species.

The third correlation between Me<sub>2</sub>N and Me<sub>3</sub>Si groups may not be expected on account of their relatively large spatial separation (crystal structure data suggest a distance of 4–5 Å). However, the fact that a considerable number of protons are involved in this specific correlation (9H from Me<sub>3</sub>Si and 6H from Me<sub>2</sub>N) might explain the observed cross-peak. The lack of correlations between DMAT and THF protons could be due to several factors. The broadness of their signal could dilute the information in the spectral noise, or the THF protons could be too “mobile” to effi-

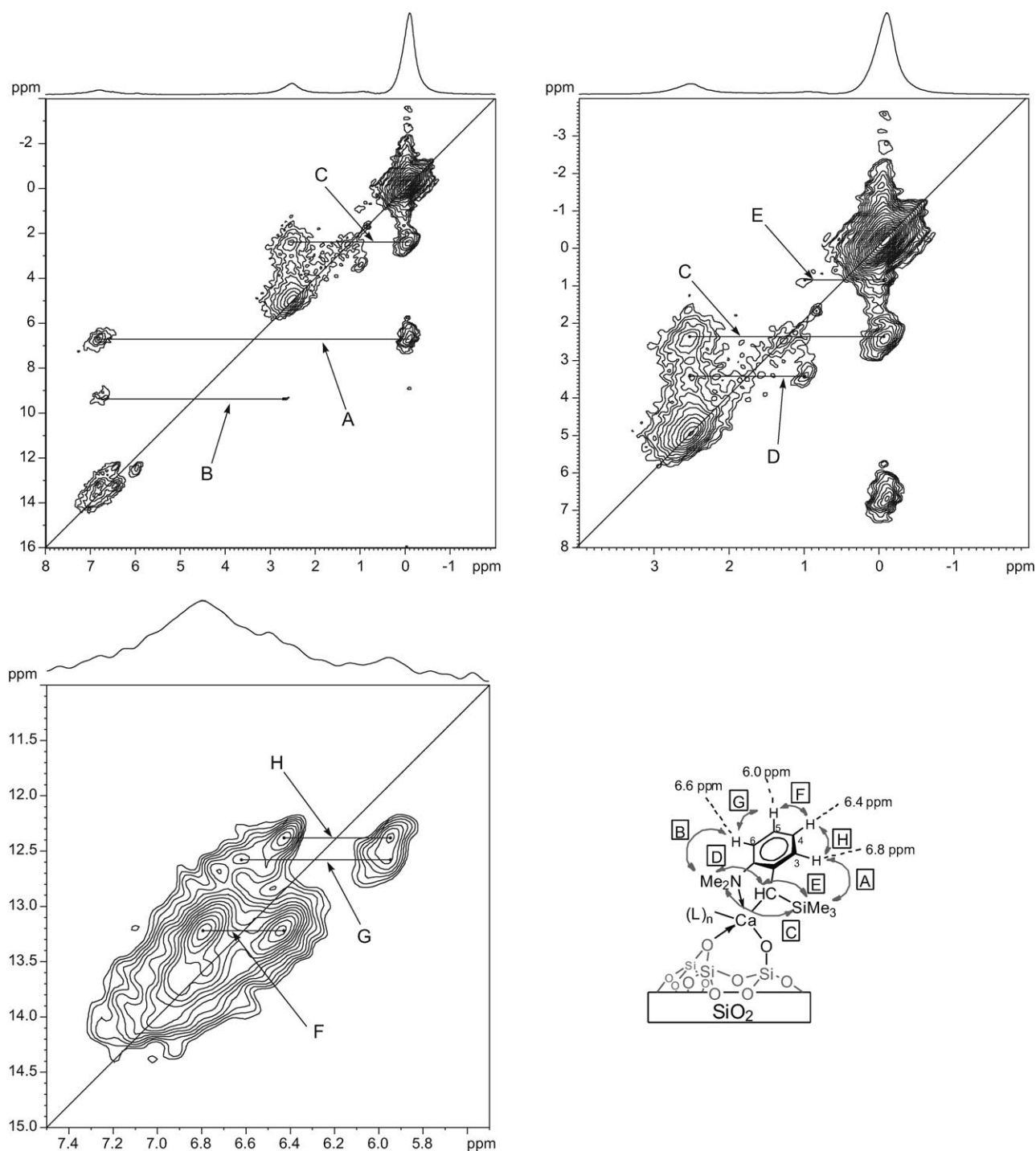


Figure 3.  $^1\text{H}$ - $^1\text{H}$  2D double quantum MAS spectrum of  $\text{SiO}_2\text{-1}$  acquired with an excitation/reconversion pulse train of four rotor periods, expanded views, and correlation assignments (800 MHz, 20 kHz spinning speed, pulse length of 2.1  $\mu\text{s}$ , 16 transients were recorded for each of the 400 t1 increments, the relaxation delay was set to 5 s).

ciently interact with others on the grafted species. This is in line with our earlier conclusions based on one-dimensional  $^1\text{H}$  NMR spectra using the BABA sequence (vide supra).

A close-up of the high-field region of the correlation spectrum reveals the presence of at least two other interactions, designated here as D and E (Figure 3, top right). These con-

cern correlations between  $\text{Me}_2\text{N}$  and  $\text{Me}_3\text{Si}$  protons with the  $\text{ArCHSiMe}_3$  proton resonating at  $\delta = 0.9$  ppm, and thus confirm its assignment. This is in agreement with the fact that no significant on-diagonal signal is detected at this chemical shift, that is, it originates from an isolated CH proton.

An enlargement of the aromatic region shows cross-peaks that allow assignment of the various signals (Figure 3, bottom left). Three main off-diagonal interactions can be observed: F, between  $\delta=6.8$  and 6.4 ppm; G, between  $\delta=6.6$  and 6.0 ppm; and H, between  $\delta=6.4$  and 6.0 ppm. We also know that an intense correlation involves the proton resonating at  $\delta=6.8$  ppm with the  $\text{Me}_3\text{Si}$  group (interaction A). A broader correlation (B, lower intensity) is observed between the low-field aromatic protons at  $\delta=6.8\text{--}6.6$  ppm (undistinguished) and the  $\text{Me}_2\text{N}$  substituent. This would allow one to assign a chemical shift of  $\delta=6.8$  ppm to the CH group *ortho* to the  $\text{CHSiMe}_3$  group ( $\text{C}^3\text{H}$ ), and of  $\delta=6.6$  ppm to the CH *ortho* to the  $\text{Me}_2\text{N}$  moiety ( $\text{C}^6\text{H}$ ). The remaining assignments can then be proposed on the basis of the three interaromatic correlations:  $\delta=6.4$  ppm for  $\text{C}^4\text{H}$  and  $\delta=6.0$  ppm for  $\text{C}^5\text{H}$ . This assignment would be in good agreement with solution data. Precursor **1** in solution (in  $\text{C}_6\text{D}_6$ ) consists of two slowly interconverting diastereomers. For the aromatic  $\text{C}^3\text{H}\text{--}\text{C}^4\text{H}\text{--}\text{C}^5\text{H}\text{--}\text{C}^6\text{H}$  part the following sets of  $^1\text{H}$  NMR signals were observed:  $\delta=7.12, 6.89, 6.38, 6.72$  and  $7.18, 6.85, 6.55, 6.27$  ppm. Both compare well to the 6.8, 6.4, 6.0, 6.6 ppm sequence proposed for the aromatic signals in **SiO<sub>2</sub>-1**.

The  $^{13}\text{C}$  CP-MAS NMR spectra of **1** and **SiO<sub>2</sub>-1** are displayed in Figure 4. The solid-state  $^{13}\text{C}$  spectrum of crystalline **1** features two sets of sharp well-resolved signals, accounting for the aromatic carbon atoms ( $\delta=149.0\text{--}110.9$  ppm), CH and  $\text{Me}_2\text{N}$  groups ( $\delta=49.6\text{--}39.2$  ppm), THF  $\alpha$ - ( $\delta=70.0$  and 68.8 ppm) and  $\beta$ -carbon atoms ( $\delta=25.8$  and 24.6 ppm), and  $\text{Me}_3\text{Si}$  moieties ( $\delta=4.5$  and 2.5 ppm). As only one of the two diastereomers of precursor **1** is found in the crystal structure (the *meso* form with *R* and *S* chirality at the benzylic carbon atoms),<sup>[6]</sup> the two sets of signals must arise from the nonsymmetry of this particular diastereomer (nonsymmetry is also observed in the crystal structure). This is confirmed by observation of a double set of signals for

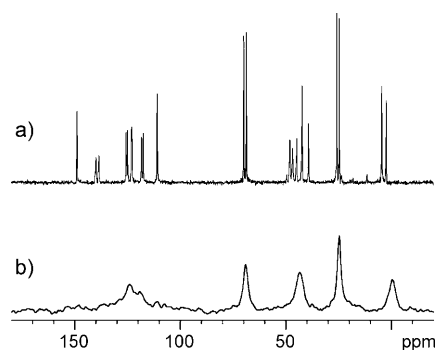


Figure 4.  $^{13}\text{C}$  CP-MAS NMR spectrum of a) **1** (64 transients) and b) **SiO<sub>2</sub>-1** (2560 transients) at 100.62 MHz with a relaxation delay of 5 s. The contact time was set to 1 ms at a radio-frequency field of 50 kHz.  $^1\text{H}$  decoupling at 90 kHz was applied during  $^{13}\text{C}$  acquisition.

the THF ligands, which indicates their different environments. In contrast, the solution spectrum of **1** is composed of a double set of signals for the DMAT ligands (indicating slow exchange between the two diastereomers) but only one set for the THF ligands (indicating fast exchange between the two different THF ligands).<sup>[6]</sup>

The  $^{13}\text{C}$  CP-MAS NMR spectrum of **SiO<sub>2</sub>-1** comprises five distinct patterns (Figure 4b). The aromatic carbon atoms resonate in the range of  $\delta=130\text{--}110$  ppm. Compared to the spectrum of the molecular precursor, the two low-field aromatic signals from the DMAT quaternary carbon atoms are not detected in the spectrum of the grafted species under these experimental conditions. The coordinated THF molecules give rise to two signals, at  $\delta=69.0$  ( $\text{C}_\alpha$ ) and 24.7 ppm ( $\text{C}_\beta$ ). The  $\text{Me}_2\text{N}$  and methyne carbon signals cannot be distinguished, as a broad peak is observed at  $\delta=43$  ppm. The  $\text{Me}_3\text{Si}$  carbon atoms resonate at  $\delta=-0.5$  ppm, which is shifted somewhat to high field compared to **1**.

The  $^1\text{H}\text{--}^{13}\text{C}$  CP HETCOR NMR spectrum of **SiO<sub>2</sub>-1** was recorded to confirm and refine the assignments (Figure 5).

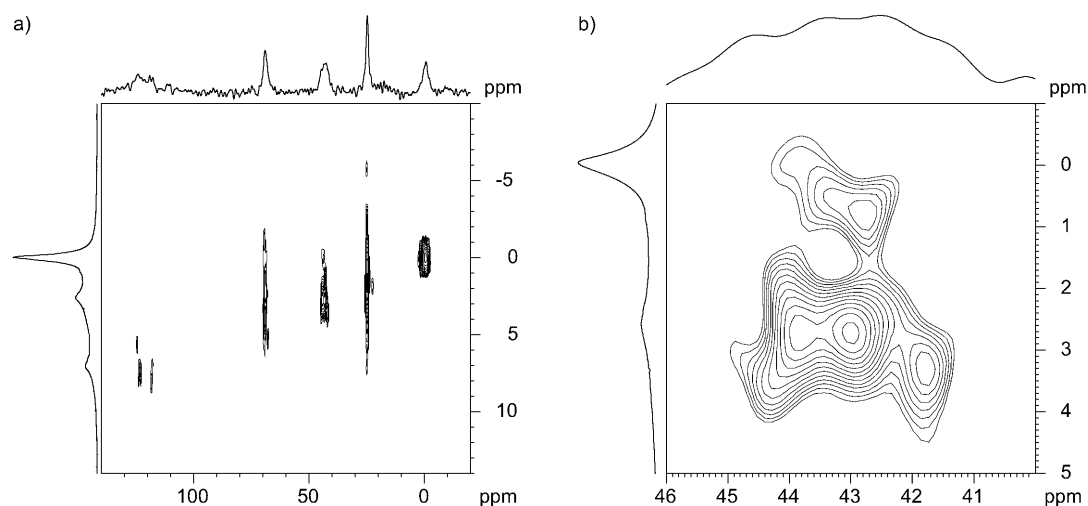


Figure 5. a)  $^1\text{H}\text{--}^{13}\text{C}$  CP HETCOR NMR spectrum of **SiO<sub>2</sub>-1**. The CP conditions are identical to those used for the spectra in Figure 4. A total of 1024 transients was added for each of the 64 t1 increments. The relaxation delay was set to 5 s. The 2D processing included an exponential line broadening of 20 Hz in both dimensions. b) Close up of the  $\text{Me}_2\text{N}$ /methyne area.

This pulse sequence includes a cross-polarization contact time to correlate carbon nuclei through space with neighboring protons. Accordingly, the spectrum comprises the expected correlations between protons and carbon atoms of the aromatic ring, of THF  $\alpha$ - and  $\beta$ -methylene groups (respective H–C couples:  $\delta=4.1/69.0$ , and  $1.5/24.7$  ppm), and of the  $\text{Me}_3\text{Si}$  fragment (H–C couple:  $\delta=0/-0.5$  ppm). As shown in Figure 5, the  $^{13}\text{C}$  signal of the  $\text{Me}_2\text{N}$  and CH groups at about  $\delta=43$  ppm gives rise to several cross-peaks. Three of them are indicative of MeN moieties in different environments, at  $\delta_{\text{H}}/\delta_{\text{C}}$  of  $3.3/41.8$ ,  $2.7/43.0$ , and  $2.7/43.8$  ppm (a maximum of four MeN signals is expected). Only in the last-named couple is residual interaction with the  $\text{Me}_3\text{Si}$  group detected, which may be an indication of the actual configuration of the silica-grafted species. However, at this stage, further refinement of the assignment appears difficult. Most interestingly, a cross-peak associates the methinic proton at  $\delta=0.9$  ppm with a signal centered at  $\delta=42.7$  ppm in the  $^{13}\text{C}$  dimension, fully in line with the observed values for the CaCH moiety in solution: the two diastereomers show  $^1\text{H}$  and  $^{13}\text{C}$  signals at  $\delta=0.89/1.24$  ppm and  $42.8/47.1$  ppm, respectively.<sup>[6]</sup>

**Reaction of  $\text{Ca}[\text{N}(\text{SiMe}_3)_2]_2 \cdot 2\text{thf}$  (**2**) with  $\text{SiO}_2\text{-700}$ : synthesis and characterization of  $\text{SiO}_2\text{-2}$ :** Reaction of **2** with  $\text{SiO}_2\text{-700}$  suspended in pentane gave, after subsequent washing with pentane and drying under high vacuum ( $10^{-6}$  mmHg), an off-white material ( $\text{SiO}_2\text{-2}$ ). Grafting of **2** onto  $\text{SiO}_2\text{-700}$  is expected to follow a similar pattern to grafting of the related lanthanide compounds  $\text{Ln}[\text{N}(\text{SiMe}_3)_2]_3$ .<sup>[14]</sup> In the latter case, the monopodal species  $(\equiv\text{SiO})\text{Ln}[\text{N}(\text{SiMe}_3)_2]_2$  is formed through protonolysis of a Ln–amido bond by a silanol group, and a concomitant side reaction was observed in which some of the silanol groups were silylated by the released  $(\text{Me}_3\text{Si})_2\text{NH}$  to give  $\equiv\text{SiOSiMe}_3$  and  $\text{NH}_3$  (via transient  $\text{Me}_3\text{SiNH}_2$ ). Thus, a silanol-free surface was obtained in fine.<sup>[15]</sup>

Elemental analysis indicates a Ca loading of 1.72 wt%, which corresponds to a surface density of 0.75 Ca per square nanometer. In comparison, grafting of  $\text{SiO}_2\text{-700}$  with  $\text{Ln}[\text{N}(\text{SiMe}_3)_2]_3$  gave only a Ln content of  $0.48 \text{ nm}^{-2}$  (Ln = Y, La, Nd, Sm). This difference most probably stems from the considerably smaller size of the grafted  $\text{CaN}(\text{SiMe}_3)_2$  group compared to the  $\text{Ln}[\text{N}(\text{SiMe}_3)_2]_3$  group. This decrease in steric hindrance for the remaining silanol groups favors further metalation versus trimethylsilylation. The modest steric bulk of the  $\text{CaN}(\text{SiMe}_3)_2$  group also explains a higher Ca loading than observed for the grafted calcium benzyl species ( $0.55 \text{ nm}^{-2}$ ). The Ca/N ratio of 0.98 is in agreement with the formation of monografted surface species  $\text{CaN}(\text{SiMe}_3)_2$ . As  $\text{SiO}_2\text{-700}$  bears 1.1 OH per square nanometer, of which 0.75 are bound to calcium, 0.35 silylated silanol groups ( $\equiv\text{SiOSiMe}_3$ ) per square nanometer should have been formed. Thus, the C/Ca ratio of 12.1 corresponds to 1.3 THF per calcium center. This is consistent with a surface species formulated as  $(\equiv\text{SiO})\text{CaN}(\text{SiMe}_3)_2 \cdot 1.3 \text{ thf}$ .

The absence of an IR band at  $3747 \text{ cm}^{-1}$ , characteristic for isolated silanol groups, indicates their complete consumption (Figure 1). Infrared signals similar to those of the molecular precursor **2** can be observed for modified silica  $\text{SiO}_2\text{-2}$  ( $\nu(\text{C-H})$  at  $2980\text{--}2800 \text{ cm}^{-1}$  and  $\delta(\text{C-H})$  at  $1480 \text{ cm}^{-1}$ ).<sup>[12]</sup> Regarding the fate of the ammonia released in the silylation side reaction, no NH-related bands ( $3380$  and  $3320 \text{ cm}^{-1}$ ) are detected, that is, coordinated  $\text{NH}_3$  is not present in the material. This also shows that the possible side reaction between  $\text{CaN}(\text{SiMe}_3)_2$  and  $\text{NH}_3$ , which could give grafted  $\text{CaNH}_2$ , did not occur under these reaction conditions.<sup>[16]</sup>

Solid-state NMR spectra of  $\text{SiO}_2\text{-2}$  display the expected features for the proposed chemical composition. The  $^1\text{H}$  MAS NMR spectrum comprises a sharp high-field signal at  $\delta=-0.73$  ppm with a shoulder at  $\delta=-0.57$  ppm (Figure 6).

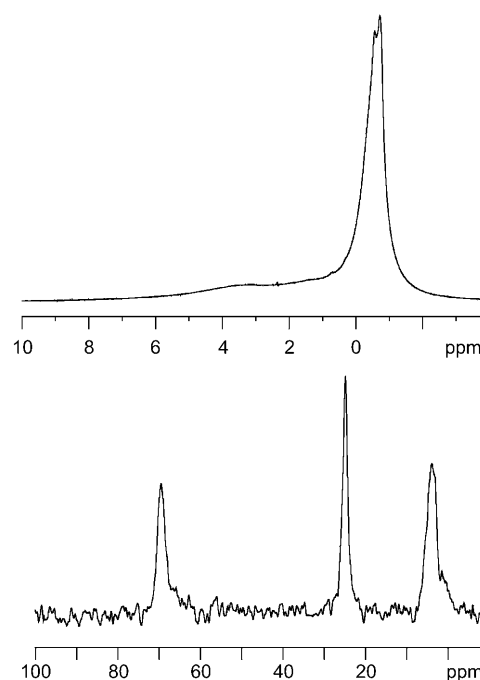


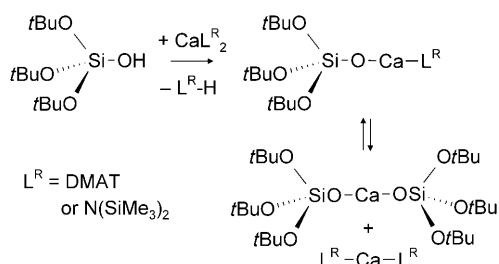
Figure 6. Top:  $^1\text{H}$  MAS NMR spectrum of  $\text{SiO}_2\text{-2}$  (400.13 MHz, 12.5 kHz spinning speed, relaxation delay of 5 s, 16 transients); bottom:  $^{13}\text{C}$  CP MAS NMR spectrum of  $\text{SiO}_2\text{-2}$  (100.62 MHz, 12.5 kHz spinning speed, 1024 transients), with a relaxation delay of 5 s. The contact time was set to 1 ms at a radio-frequency field of 50 kHz.  $^1\text{H}$  decoupling at 80 kHz was applied during the  $^{13}\text{C}$  acquisition.

These signals are assigned to the  $\text{Me}_3\text{Si}$  groups of the  $\text{N}(\text{SiMe}_3)_2$  and  $\equiv\text{SiOSiMe}_3$  units, respectively. Broad signals due to the THF ligands are observed at  $\delta=3.17$  and  $1.3$  ppm, whereby the latter is partially masked by the  $\text{Me}_3\text{Si}$  peaks.

Accordingly, the  $^{13}\text{C}$  CP-MAS NMR spectrum comprises three main peaks at  $\delta=3.8$ ,  $24.8$ , and  $69.5$  ppm which correspond to  $\text{Me}_3\text{Si}$  and the  $\beta$ - and  $\alpha$ -carbons of calcium-bound THF moieties, respectively (Figure 6). Noteworthy, a high-field shoulder on the  $\text{Me}_3\text{Si}$  signal may be indicative of  $\equiv\text{SiOSiMe}_3$ . The concomitant presence of  $\text{CaNSiMe}_3$  and

$\equiv\text{SiOSiMe}_3$  groups was confirmed by observation of the expected  $^{29}\text{Si}$  CP-MAS NMR signals at  $\delta = -13.4$  and  $12.4$  ppm, respectively.<sup>[12,15,17]</sup>

**Molecular model of grafted calcium catalysts:** The heterogeneous character of the grafted calcium amide and benzyl species prevents a detailed study on their bonding situation. As insights into the possible bonding modes involving the silyl ether-rich silica surface and the metal would afford a better understanding of the supported species, we investigated the synthesis and structural characterization of a model system. A molecular ligand that mimics the isolated silanol functionality on the surface of  $\text{SiO}_2\text{-700}$  is the bulky ether-rich silanol  $(t\text{BuO})_3\text{SiOH}$ .<sup>[18]</sup> Reaction of  $(t\text{BuO})_3\text{SiOH}$  with  $\text{Ca}(\text{DMAT})_2 \cdot 2\text{thf}$  (**1**) or  $\text{Ca}[\text{N}(\text{SiMe}_3)_2]_2 \cdot 2\text{thf}$  (**2**) could give a surface-like heteroleptic complex (Scheme 3).



Scheme 3.

The equimolar reaction of either **1** or **2** with  $(t\text{BuO})_3\text{SiOH}$  was monitored by  $^1\text{H}$  NMR. The sharp silanol peaks changed to broad signals, indicative of slow exchange. More importantly, even though the correct 1/1 stoichiometry was used, in both cases half of the calcium reagent did not react. Apparently, the Schlenk equilibrium is fully to the side of the homoleptic complexes (Scheme 3). This underscores the importance of grafting as a tool in the syntheses of heteroleptic calcium reagents.

The homoleptic complex  $\text{Ca}[\text{OSi}(t\text{BuO})_3]_2$  could be prepared in quantitative yield by reaction of **2** with two equivalents of the bulky silanol. The product that remains after removing all volatile materials is extremely soluble in pentane, and even at  $-80^\circ\text{C}$  no crystals could be obtained. After three weeks at room temperature, however, large colorless crystalline blocks started to separate. The crystal structure showed a complex of composition  $[\text{Ca}^{2+}]_4[(t\text{BuO})_3\text{SiO}^-]_6[\text{OH}^-]_2 \cdot \text{thf}$ . The presence of an isolated  $\text{OH}^-$  ligand was confirmed by the observation of a relatively sharp IR signal at  $3675\text{ cm}^{-1}$ , typical for calcium hydroxide complexes (a recently reported dimeric  $\beta$ -diketiminato calcium hydroxide complex showed an IR signal at  $3697\text{ cm}^{-1}$ ).<sup>[19]</sup> Apparently the long crystallization time caused partial hydrolysis to give a less soluble siloxide-hydroxide cluster.

The crystal structure of this cluster is shown in Figure 7, and selected interatomic distances are summarized in Table 1. The framework of the structure can be best described as two fused  $\text{Ca}/\text{O}$  cubes with two missing corners.

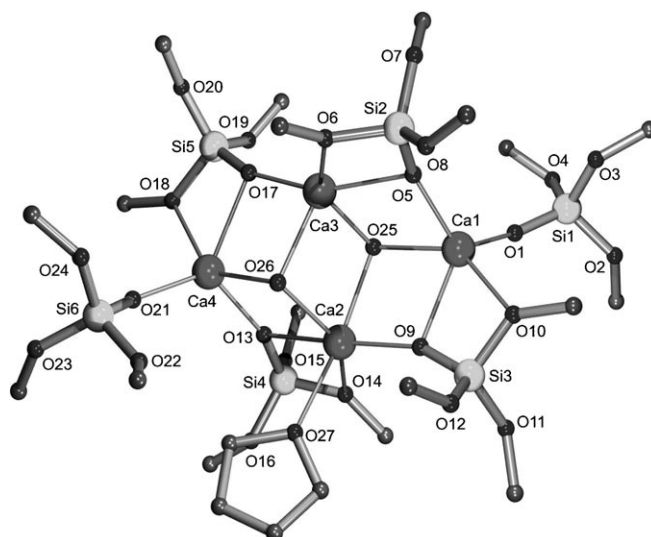


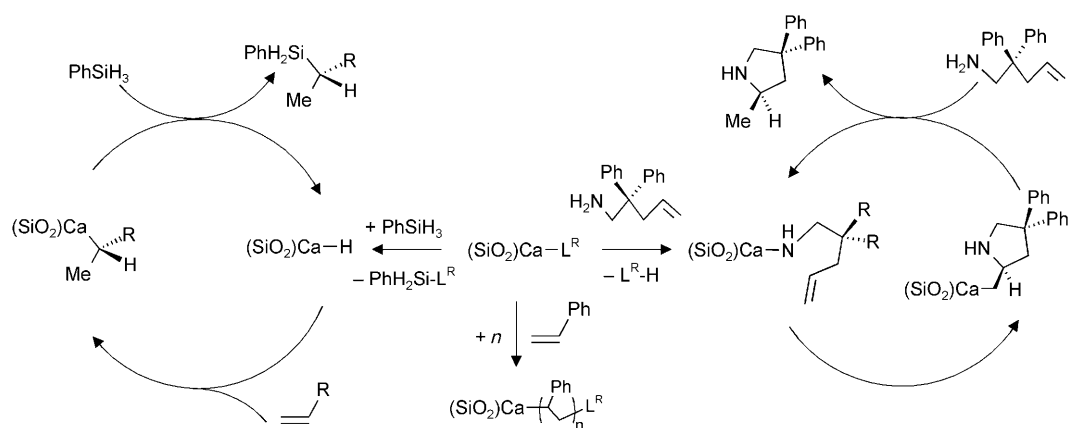
Figure 7. Crystal structure of  $[\text{Ca}^{2+}]_4[(t\text{BuO})_3\text{SiO}^-]_6[\text{OH}^-]_2 \cdot \text{thf}$ ; hydrogen atoms and methyl groups ( $t\text{Bu}$ ) have been omitted for clarity.

Table 1. Selected interatomic distances [ $\text{\AA}$ ] in the crystal structure of  $[\text{Ca}^{2+}]_4[(t\text{BuO})_3\text{SiO}^-]_6[\text{OH}^-]_2 \cdot \text{thf}$ .

Ca1–O1	2.128(4)	Ca2–O14	2.435(3)	Ca3–O25	2.288(3)
Ca1–O5	2.264(3)	Ca2–O25	2.345(5)	Ca3–O26	2.269(5)
Ca1–O9	2.390(5)	Ca2–O26	2.340(3)	Ca4–O13	2.227(3)
Ca1–O10	2.429(4)	Ca2–O27	2.386(7)	Ca4–O17	2.452(5)
Ca1–O25	2.366(3)	Ca3–O5	2.411(3)	Ca4–O18	2.416(4)
Ca2–O9	2.283(3)	Ca3–O6	2.410(3)	Ca4–O21	2.165(4)
Ca2–O13	2.427(3)	Ca3–O17	2.244(3)	Ca4–O26	2.380(3)

The approximate  $C_i$  symmetry is broken by coordination of a THF ligand to  $\text{Ca}2$ . This structure type is also found in a recently published aryloxy hydroxide calcium cluster of composition  $[\text{Ca}^{2+}]_4[\text{ArO}^-]_6[\text{OH}^-]_2$ , which was obtained by controlled hydrolysis of  $\text{Ca}(\text{OAr})_2$ .<sup>[20]</sup> This particular framework, which also has been observed in several other crystal structures of aryloxy calcium complexes, must be a highly favored structural type.<sup>[21]</sup> As suggested, the  $[\text{M}^{2+}]_4[\text{RO}^-]_6[\text{OH}^-]_2$  arrangement is likely an important intermediate in the hydrolysis of molecular species in sol-gel applications.<sup>[20]</sup>

The cluster contains two terminal  $(t\text{BuO})_3\text{SiO}^-$  ligands, while the other four bridge two  $\text{Ca}^{2+}$  ions. All bridging ligands show additional coordination of a  $t\text{BuO}$  side arm to one of the  $\text{Ca}^{2+}$  ions. The  $\text{Ca}-\text{O}$  bonds for terminal ligands ( $2.128(4)$ – $2.165(4)$   $\text{\AA}$ ) are shorter than those for bridging ligands ( $2.244(3)$ – $2.452(5)$   $\text{\AA}$ ). The terminal and bridging  $\text{Ca}-\text{O}$  bond lengths compare well to those in a recently published silsesquioxane calcium complex.<sup>[22]</sup> The  $\text{Ca}-\text{O}$  bonds to the ether side arms are generally the longest ( $2.410(3)$ – $2.435(3)$   $\text{\AA}$ ), but still significantly shorter than those in the silsesquioxane calcium complex ( $2.635(3)$ – $2.844(4)$   $\text{\AA}$ ).<sup>[22]</sup> The crystal structure nicely shows the variety of bonding modes that could play a role in silica-grafted organocalcium species.



Scheme 4. Catalytic applications of grafted calcium catalysts.

**Preliminary catalytic studies on SiO<sub>2</sub>-1 and SiO<sub>2</sub>-2:** To explore the scope of silica-grafted calcium amide and benzyl groups in catalysis, we investigated their catalytic activity in the hydrosilylation of activated alkenes, intramolecular alkene hydroamination, and in styrene polymerization (proposed catalytic cycles are shown in Scheme 4; L<sup>R</sup> represents the reactive ligand DMAT or N(SiMe<sub>3</sub>)<sub>2</sub>).

Ca(DMAT)<sub>2</sub>·2thf has been shown to be an effective catalyst in the homogeneous hydrosilylation of conjugated alkenes.<sup>[4e]</sup> Apart from considerable activity, it also showed very good regioselectivity. In some cases the regioselectivity could be controlled conveniently by choice of solvent or by switching to more polar catalysts (based on Sr or K).<sup>[4e]</sup> Also Ca[N(SiMe<sub>3</sub>)<sub>2</sub>]<sub>2</sub>·2thf shows good activity in this highly atom efficient key transformation.<sup>[4f]</sup>

Supported catalysts **SiO<sub>2</sub>-1** and **SiO<sub>2</sub>-2** were tested in the hydrosilylation of styrene, cyclohexadiene, and 1,1-diphenylethylene (DPE) with PhSiH<sub>3</sub>. The results are compared with those of the ungrafted catalysts under homogeneous conditions (Table 2). The reactions were carried out with 5 mol% catalyst loading (based on active groups) in benzene or THF at temperatures ranging from 20 to 50 °C. The conversion of substrates to products was monitored by <sup>1</sup>H NMR spectroscopy. The following conclusions can be drawn: 1) In all cases initiation of the catalyst takes place by reaction of (SiO<sub>2</sub>)<sub>2</sub>CaL<sup>R</sup> with PhSiH<sub>3</sub>. The product PhH<sub>2</sub>SiL<sup>R</sup> could be detected, and presumably the actual catalyst is a grafted calcium hydride: (SiO<sub>2</sub>)<sub>2</sub>CaH (Scheme 4). 2) The observed conversions after a given time are in most cases similar to or slightly lower than those found under homogeneous conditions. An exception is found for DPE, the most sterically hindered alkene, which under homogeneous conditions also reacts more slowly than styrene or cyclohexadiene (at least under apolar conditions). 3) Similar to runs under homogeneous conditions, the regioselectivity for the hydrosilylation of DPE depends on the polarity of the solvent: in an apolar medium exclusively branched products are formed (Table 2, entries 5 and 6), whereas in THF the linear silanes were obtained (Table 2, entries 7 and 8). Formation of the latter should be explained by an alternative mechanism.<sup>[4e]</sup>

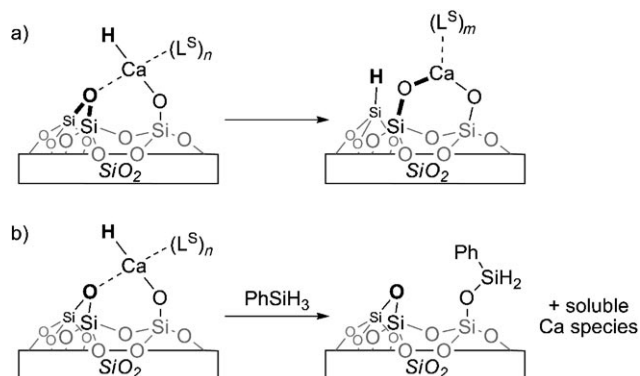
Table 2. Catalytic hydrosilylation of activated alkenes by PhSiH<sub>3</sub>.<sup>[a]</sup>

Entry	Substrate	Product	Catalyst	T [°C]	t [h]	Conversion [%] <sup>[b]</sup>
1			<b>SiO<sub>2</sub>-1</b>	20	< 0.1	> 98
			<b>1</b>	20	< 0.1	> 98
2			<b>SiO<sub>2</sub>-2</b>	50	1	> 98
			<b>2</b>	50	1	> 98
3			<b>SiO<sub>2</sub>-1</b>	50	1.5	> 98
			<b>1</b>	20	< 0.1	> 98
4			<b>SiO<sub>2</sub>-2</b>	50	2 (16)	93 (98)
			<b>2</b>	50	1	> 98
5			<b>SiO<sub>2</sub>-1</b>	50	0.5 (36)	35 (47)
			<b>1</b>	50	16	> 98
6			<b>SiO<sub>2</sub>-2</b>	50	1 (24)	30 (63)
			<b>2</b>	50	1	> 98
7 <sup>[c]</sup>			<b>SiO<sub>2</sub>-1</b>	50	2	> 98
			<b>1</b>	50	3	> 98
8 <sup>[c]</sup>			<b>SiO<sub>2</sub>-2</b>	50	3	> 98

[a] General conditions: 0.5 mmol alkene, 0.5 mmol PhSiH<sub>3</sub>, 300 mg solvent, catalyst concentration calculated per active Ca amide or Ca benzyl fragment: **1** and **2** (0.025 mmol), **SiO<sub>2</sub>-1** (0.026 mmol), and **SiO<sub>2</sub>-2** (0.036 mmol). [b] Measured by NMR spectroscopy. [c] Solvent = [D<sub>8</sub>]THF.

The catalytic activity of **SiO<sub>2</sub>-1** and **SiO<sub>2</sub>-2** in the hydrosilylation of alkenes shows that the silica surface bears reactive calcium benzyl and amide functionalities. However, it is hitherto unclear whether catalysis proceeds in a homogeneous or heterogeneous fashion. The fact that bulky substrates like DPE react considerably more slowly with silica-grafted catalysts is an indication for a heterogeneous process. During the catalytic hydrosilylation of DPE, the solid catalyst turns bright red, whereas the solvent (benzene or THF) is colorless. This is a strong indication for a (≡SiO)CaC-(Me)Ph<sub>2</sub> resting state.

As even prolonged reaction times never lead to full conversion in the hydrosilylation of DPE, for slower reactions catalyst decomposition can be an issue. A possible route for catalyst decomposition could be reaction of the proposed surface hydride ( $\equiv\text{SiO}-\text{CaH}\cdot n\text{thf}$ ) with a  $\equiv\text{Si}-\text{O}-\text{Si}\equiv$  bond of the silica to give  $(\equiv\text{SiO})_2\text{Ca}\cdot n\text{thf}$  and  $\equiv\text{SiH}$  (Scheme 5 a).



Scheme 5. Proposed reaction paths accounting for surface hydride deactivation.

Cleavage of the  $\equiv\text{SiO}-\text{Ca}(\text{L}^{\text{R}})$  bond by  $\text{PhSiH}_3$  to give  $\equiv\text{SiO}-\text{SiH}_2\text{Ph}$  and  $\text{HCa}(\text{L}^{\text{R}})$  may also be envisioned (Scheme 5 b). However, in the latter case a soluble calcium hydride would be released from the surface and higher catalytic activity should be observed.

In the case of entry 5 (Table 2), reloading an isolated and washed  $\text{SiO}_2\text{-1}$  catalyst with substrates gave further conversion, although at a much lower rate (20% after 30 h). This could be either due to catalyst deactivation (Scheme 5 a) or cleavage (Scheme 5 b). Analysis of the used catalyst by IR and MAS NMR spectroscopy show indications for formation of  $\equiv\text{SiH}$  surface species, but not  $\equiv\text{SiO}-\text{SiH}_2\text{Ph}$ .<sup>[12]</sup> Therefore, catalyst deactivation is the more likely decomposition route.

The proposed catalyst in the hydrosilylation of alkenes is a monomeric surface hydride, which is expected to be highly reactive. Calcium-mediated intramolecular hydroamination of aminoalkenes<sup>[4e, g, i]</sup> proceeds through a calcium amido intermediate (Scheme 4), which should be much less reactive and less prone to decomposition. We investigated the intramolecular hydroamination of  $\text{H}_2\text{C}=\text{CHCH}_2\text{C}(\text{Ph})_2\text{CH}_2\text{NH}_2$  and found that catalyst  $\text{SiO}_2\text{-2}$  catalyzes ring closure to give the expected product (90% after 16 h, 10 mol% cat.,  $\text{C}_6\text{D}_6$ , 20°C). This is considerably slower than under homogeneous conditions with catalyst **2** (>98% after 1 h, 10 mol% cat.,  $\text{C}_6\text{D}_6$ , 20°C). Apparently the ring-closure process on the silica surface is sterically hindered. Neither the isolated catalyst nor the mother liquor is catalytically active towards a second loading of substrate. There is, however, an indication that the catalytic reaction is heterogeneous. A used catalyst was isolated, washed, and suspended in  $\text{C}_6\text{D}_6$ . Addition of  $\text{CD}_3\text{OD}$  led to immediate appearance of  $^1\text{H}$  NMR signals for the ring-closure product. From quantification of the

product released we can conclude that 44% of all initial active sites bind a cyclic amide. As we could not detect a coupling pattern for  $\text{CH}_2\text{D}$ , it is likely that the catalytic intermediate in Scheme 4 isomerizes by a 1,3-H shift to a more stable calcium amide complex, which is released after  $\text{CD}_3\text{OD}$  addition. We did not find any released substrate  $\text{H}_2\text{C}=\text{CHCH}_2\text{C}(\text{Ph})_2\text{CH}_2\text{NH}_2$  on addition of  $\text{CD}_3\text{OD}$ . Therefore, it is likely that the product was chemically bound to the surface and not physisorbed, as in this case desorbed products would also comprise a fraction of unconverted substrate bearing in mind the conversion of 90%.

The grafted benzyl calcium catalyst was also investigated in the polymerization of styrene. Earlier work showed that benzyl calcium complexes are efficient initiators for living polymerization of styrene.<sup>[4a]</sup> Whereas the homoleptic calcium catalyst  $\text{Ca}(\text{DMAT})_2\cdot 2\text{thf}$  (**1**) gives largely atactic polystyrene, polymer obtained with the heteroleptic initiator  $\text{Ca}(\text{DMAT})(9\text{-Me}_3\text{Si-fluorenyl})\cdot\text{thf}$  shows a remarkable syndiotacticity which strongly depends on the styrene concentration (in pure styrene 92% *r* diads are found).<sup>[23]</sup> Recently, we found that extending the fluorenyl ligand by substitution at the 2- and 7-positions gave a large increase in tacticity control: even under dilute conditions syndiotacticities up to 92% (*r* diads) were found.<sup>[24]</sup> As the silica surface can be seen as a very extensive ligand, efficient tacticity control in styrene polymerization is expected.

Polymerization of styrene with the initiator  $\text{SiO}_2\text{-1}$  was either performed in solution (10% styrene in cyclohexane, 50°C) or in the bulk (100% styrene, 20°C). Whereas solution polymerizations with initiator **1** give full conversion of monomer within 30 min, polymerization with grafted initiator  $\text{SiO}_2\text{-1}$  is considerably slower. After one hour only 4% polymer could be isolated. Polymerization over 20 h gave 18% conversion. The much slower polymerization rates are likely due to the fact that monomer transport to the surface-bound active sites is increasingly hindered by the growing polymer chains. The obtained polymer also shows a somewhat broadened molecular weight distribution ( $M_n=1.68\times 10^4$ ,  $\text{PDI}=1.45$ )<sup>[12]</sup> indicative of different active sites during polymerization. Analysis by  $^{13}\text{C}$  NMR spectroscopy, however, revealed a considerable syndiotacticity of 88% (*r* diads). These observations all point to a heterogeneous polymerization reaction, as leaching of the grafted catalyst would give essentially atactic polystyrene.

Polymerization in neat styrene gave a polymer with a bimodal molecular weight distribution, the main fraction of which was a polymer with an  $M_n$  of  $1\times 10^5\text{ g mol}^{-1}$ , whereas the smaller fraction shows an extremely high  $M_n$  value of  $2\times 10^6\text{ g mol}^{-1}$ .<sup>[12]</sup> We assign the high molecular weight fraction to leaching of a small part of the catalyst into the solution to give a homogeneous propagating species which can grow rapidly. The  $^{13}\text{C}$  NMR analysis of the polymer confirms involvement of at least two propagating species: the signal intensities do not follow Bernoullian statistics. Instead signals for a polymer of considerable syndiotacticity (from heterogeneous polymerization) overlap with signals from a fully atactic polymer (from homogeneous polymerization). Be-

cause styrene is less easy to dry than cyclohexane, leaching of the propagating species might proceed by reaction with water. This could generate mobile  $\text{Ca}(\text{OH})_2$  which, in Schlenk equilibrium with a grafted propagating species, could form mobile growing chains.

## Conclusion

Homoleptic calcium benzyl or silylamide reagents react readily with isolated surface silanol groups of partially dehydrated silica. Appropriate support pretreatment allows selective formation of monopodal, heteroleptic species ( $\equiv \text{SiO})\text{Ca}(\text{L}^{\text{R}})_n\text{thf}$  with a reactive calcium–ligand bond and a spectator  $\text{SiO}-\text{Ca}$  linkage. Due to the bulk of these calcium-based fragments, full coverage of the surface is not reached. Whereas unconverted residual silanol groups are still present on the surface after grafting of the benzyl derivative, complete capping with trimethylsilyl groups is observed in the amido case. The grafted calcium benzyl and amide fragments have been characterized with a variety of analytical methods (IR, 1D, and 2D solid-state NMR, elemental analysis).

Preliminary results show that the grafted calcium benzyl and amide groups are active in catalytic hydrosilylation of alkenes and intramolecular hydroamination of alkenes. Although recycling of the catalysts was not very efficient, key experiments demonstrate that reactions were catalyzed by supported calcium species. Moreover, grafted calcium benzyl species can be used to initiate styrene polymerization. Simple grafting of the homoleptic initiator  $\text{Ca}(\text{DMAT})_2 \cdot 2\text{thf}$  (**1**), which produces mostly atactic polystyrene, gave a heterogeneous initiator that produced polystyrene of considerable syndiotacticity, albeit at the expense of lower activity. This demonstrates the potential of grafting as a simple tool to enforce higher selectivity in catalytic transformations.

The intended synthesis of a molecular model system for the grafted species did not give the heteroleptic product, but instead ligand exchange in solution resulted in formation of homoleptic products. This emphasizes the fact that grafting of organocalcium reagents on the silica surface successfully prevented formation of homoleptic species by the Schlenk equilibrium. Thus, grafting could be a powerful new method in the organometallic chemistry of the heavier alkaline-earth metals Ca, Sr, and Ba, which is often plagued by Schlenk equilibria. It could also prevent aggregation and thus enable the syntheses of more reactive monomeric alkaline earth metal reagents.

## Experimental Section

**General considerations:** Manipulations were carried out under an argon atmosphere in a glove box or by using Schlenk techniques. Solvents were dried with conventional reagents and stored in a glove box over 3 Å molecular sieves. Solution NMR analyses were run on a Bruker Avance 300

spectrometer. Solid-state MAS NMR spectra were recorded on a Bruker Avance 400 spectrometer ( $^1\text{H}$ : 400.13 MHz,  $^{13}\text{C}$ : 100.62 MHz) and Avance II 800 ( $^1\text{H}$ : 800.13 MHz). Chemical shifts are given with respect to TMS for  $^1\text{H}$  and  $^{13}\text{C}$ . Proton decoupling was performed by using the SPINAL64 composite pulse sequence.<sup>[25]</sup> Diffuse-reflectance infrared spectra were collected by using a Harrick cell on a Nicolet Avatar spectrometer fitted with a MCT detector. Elemental analyses were carried out at the Service Central d'Analyse du CNRS (Ca), and in the Service d'Analyse Élémentaire, LSEO, Université de Bourgogne (C, H, N). Aerosil 380 silica (Degussa, specific area  $380\text{ m}^2\text{ g}^{-1}$  prior to heat treatment) was heated under secondary vacuum ( $10^{-6}\text{ mmHg}$ ) at  $500^\circ\text{C}$  over 15 h followed by 4 h of heating at  $700^\circ\text{C}$  (designated here as  $\text{SiO}_2\text{-700}$ ), and stored in a glove box. The starting materials  $\text{Ca}(\text{DMAT})_2 \cdot 2\text{thf}$ ,<sup>[6]</sup>  $\text{Ca}[\text{N}(\text{SiMe}_3)_2]_2 \cdot 2\text{thf}$ ,<sup>[7]</sup> 1-amino-2,2-diphenyl-pent-4-ene,<sup>[26]</sup> and  $(t\text{BuO})_3\text{SiOH}$ <sup>[18b]</sup> were prepared according to reported procedures.

**Synthesis of  $\text{SiO}_2\text{-1}$ :** In a glove box, one leg of a double-Schlenk apparatus was loaded with molecular precursor **1** (555 mg,  $9.3 \times 10^{-4}\text{ mol}$ ) dissolved in 20 mL of toluene. The other leg was charged with  $\text{SiO}_2\text{-700}$  (1.0 g) suspended in 15 mL of toluene. The yellow solution of **1** was added to the silica support by filtering through the sintered glass separating the two Schlenk tubes. The reaction mixture was stirred for 15 h at room temperature. The supernatant liquid was then separated by filtration into the other leg, from which toluene was transferred by trap-to-trap distillation back into the leg containing the modified support in order to wash away residual molecular precursor. This operation was repeated four times until colorless washing fractions were obtained. The resulting yellow powder **SiO<sub>2</sub>-1** was then dried under secondary vacuum ( $3.10^{-6}\text{ mmHg}$ ) at  $40^\circ\text{C}$  for 6 h. Elemental analysis (% , average of two measurements): C 8.19, H 1.17, N 0.51, Ca 1.26. The amount of DMAT-H released during grafting was quantified by the following procedure: in a glove box, an NMR tube was loaded with  $\text{SiO}_2\text{-700}$  (38 mg), ferrocene (6.5 mg,  $34.9\text{ }\mu\text{mol}$ ), and **1** (15 mg,  $25.1\text{ }\mu\text{mol}$ ). The sample was then sealed and vigorously shaken. Due to the orange coloration from ferrocene, no color change could be observed. After deposition of the suspended silica, the  $^1\text{H}$  NMR spectrum was recorded (no further evolution was observed). From the relative integration of the protons of ferrocene and of the  $\text{SiMe}_3$  groups of DMAT-H (100:32), it can be calculated that  $12.4\text{ }\mu\text{mol}$  of **1** reacted with silica, which corresponds to a mass of calcium of 0.50 mg. Considering the initial mass of  $\text{SiO}_2$ , this gives a Ca loading of 1.29 wt %.

**Synthesis of  $\text{SiO}_2\text{-2}$ :** White material **SiO<sub>2</sub>-2** was prepared by the procedure described above for **SiO<sub>2</sub>-1** from molecular precursor **2** (500 mg,  $9.9 \times 10^{-4}\text{ mol}$ ) and  $\text{SiO}_2\text{-700}$  (1.15 g). Elemental analysis (% , average of two measurements): C 6.23, H 1.32, N 0.59, Ca 1.72.

**Synthesis of  $[\text{Ca}^{2+}]_4[(t\text{BuO})_3\text{SiO}^-]_4[\text{OH}^-]_2\text{thf}$ :**  $(t\text{BuO})_3\text{SiOH}$  (40 mg, 0.15 mmol) was added to a solution of  $\text{Ca}[\text{N}(\text{SiMe}_3)_2]_2 \cdot 2\text{thf}$  (38 mg, 0.075 mmol) in 0.50 mL of  $\text{C}_6\text{D}_6$ . After 30 min full conversion of  $\text{Ca}[\text{N}(\text{SiMe}_3)_2]_2 \cdot 2\text{thf}$  was observed in the NMR spectra. The solvents were removed by vacuum evaporation and the remaining precipitate was dried under high vacuum and dissolved in small amounts of pentane. After 20 days the product was isolated in the form of large, slightly yellow, crystalline blocks (yield: 27 mg, 59 %). M.p.  $153^\circ\text{C}$  (decomp).  $^1\text{H}$  NMR (300 MHz,  $\text{C}_6\text{D}_6$ ,  $20^\circ\text{C}$ ):  $\delta = 3.68$  (m, 4H; thf), 1.53 (brs, 172H;  $(t\text{BuO})_3\text{SiO}$ ), 1.73 ppm (m, 4H; thf); the OH signals could not be observed, likely on account of their low intensity (2H) and broad character;  $^{13}\text{C}$  NMR (75 MHz,  $\text{C}_6\text{D}_6$ ,  $20^\circ\text{C}$ ):  $\delta = 32.4$  ( $\text{C}(\text{CH}_3)_3$ ), 73.4 ppm ( $\text{C}(\text{CH}_3)_3$ ); IR (Nujol):  $\tilde{\nu} = 3675$  (OH), 1193, 976,  $699\text{ cm}^{-1}$ ; elemental analysis calcd (%) for  $\text{C}_{76}\text{H}_{172}\text{Ca}_4\text{O}_{27}\text{Si}_6$  (1847.0): C 49.42, H 9.39; found: C 48.72, H 9.12.

**General procedure for catalytic hydrosilylation of alkenes:** All alkene substrates were dried by stirring over freshly ground  $\text{CaH}_2$  overnight. In a dry Schlenk tube 83 mg of the catalyst (**SiO<sub>2</sub>-1** ( $0.315\text{ mmol g}^{-1}$ ):  $0.026\text{ mmol}$ ; **SiO<sub>2</sub>-2** ( $0.430\text{ mmol g}^{-1}$ ):  $0.036\text{ mmol}$ ) was suspended in 300 mg of  $\text{C}_6\text{D}_6$  (or  $[\text{D}_8]\text{THF}$ ). Subsequently,  $\text{PhSiH}_3$  (0.5 mmol) and the alkene substrate (0.5 mmol) were added and the resulting suspension was stirred and heated to  $50^\circ\text{C}$ . Generally, a color change to red was observed at the beginning of the reaction. The conversion was followed by

taking samples at regular time intervals and analyzing them by  $^1\text{H}$  NMR spectroscopy and GC/MS (see Supporting Information).

**Procedure for catalytic intramolecular hydroamination:** 1-Amino-2,2-diphenylpent-4-ene was dried overnight by stirring a solution in hexane at  $60^\circ\text{C}$  on freshly ground  $\text{CaH}_2$ . In a dry Schlenk tube the catalyst ( $\text{SiO}_2\text{-2}$  (166 mg,  $0.430\text{ mmol g}^{-1}$ , 0.072 mmol) was suspended in  $\text{C}_6\text{D}_6$  (600 mg) and 1-amino-2,2-diphenylpent-4-ene (0.5 mmol) was added. The conversion was followed by taking samples at regular time intervals and analyzing them by  $^1\text{H}$  NMR spectroscopy (see the Supporting Information). In one experiment after full conversion ( $>98\%$ ) the solid catalyst was separated, washed with hexane once, and dried under high vacuum. The dried catalyst was suspended in  $\text{C}_6\text{D}_6$  together with cyclohexane as an internal standard. After recording a  $^1\text{H}$  NMR spectrum, the sample was quenched with  $\text{CD}_3\text{OD}$ . The  $^1\text{H}$  NMR spectrum of the quenched sample showed the appearance of the product signals.

**Procedure for the polymerization of styrene:** Polymerization of styrene was performed in a thermostated 100 mL stainless steel Büchi reactor at normal pressure in cyclohexane (1 M styrene solution, 1 mM catalyst  $\text{SiO}_2\text{-1}$  based on reactive DMAT groups,  $50^\circ\text{C}$ ) or in pure styrene (1 mM catalyst  $\text{SiO}_2\text{-1}$  based on reactive DMAT groups,  $20^\circ\text{C}$ ). The reactor was loaded with dry cyclohexane (90 mL, dried with  $\text{CaH}_2$  and distilled from  $n\text{BuLi}$ ) and dry styrene (11.5 mL, ca. 100 mmol, freshly distilled from  $\text{CaH}_2$  and stored over alox pearls). A suspension of the initiator  $\text{SiO}_2\text{-1}$  (317 mg, 0.1 mmol in 1 mL cyclohexane) was added via a port. The usual appearance of a red color indicated that the polymerization started immediately. After a given polymerization time (between 1 and 20 h), the mixture was quenched with oxygen-free methanol. Evaporation of all solvents and drying under high vacuum (0.01 Torr,  $120^\circ\text{C}$ , 2 h) yielded the polymer. The polymers were analyzed by GPC and  $^{13}\text{C}$  NMR spectroscopy ( $[\text{D}_2]$ tetrachloroethane). The tacticity of the polymer was checked by analyzing the  $^{13}\text{C}$  NMR signal for  $\text{C}_{\text{ipso}}$  in the phenyl ring.<sup>[12,23]</sup>

**Crystal structure of  $[\text{Ca}^{2+}]_4[(t\text{BuO})_3\text{SiO}]_4[\text{OH}]_2(\text{thf})$ :** X-ray diffraction data were measured on a Siemens SMART CCD diffractometer at  $-70^\circ\text{C}$ , and the structure solved with SHELXS-97<sup>[27]</sup> and refined with SHELXL-97<sup>[28]</sup> PLATON<sup>[29]</sup> was used for geometry calculations and graphics. Crystal data:  $\text{C}_{76}\text{H}_{172}\text{Ca}_4\text{O}_{27}\text{Si}_6$ ,  $M_r=1847.04$ , triclinic, space group  $P1$ ,  $a=14.0780(13)$ ,  $b=14.8270(13)$ ,  $c=15.6881(15)$  Å,  $\alpha=92.338(5)$ ,  $\beta=107.983(5)$ ,  $\gamma=117.059(5)^\circ$ ,  $V=2709.5(5)$  Å<sup>3</sup>,  $Z=1$ ,  $\rho_{\text{calcd}}=1.131\text{ Mg m}^{-3}$ ,  $F(000)=1006$ ,  $\mu(\text{MoK}\alpha)=0.328\text{ mm}^{-1}$ . Of the 53379 measured reflections, 22610 were independent ( $R_{\text{int}}=0.036$ ,  $\theta_{\text{max}}=27.7^\circ$ ) and 18252 observed [ $I>2\sigma(I)$ ]. The final refinement converged to  $R1=0.0696$  for [ $I>2\sigma(I)$ ],  $wR2=0.2064$ , and  $\text{GOF}=0.99$  for all data. The final difference Fourier synthesis gave min./max. residual electron density of  $-0.57/+0.71\text{ e}\text{Å}^{-3}$ . All hydrogen atoms were placed on calculated positions and were refined in a riding mode. The structure was refined as an inversion twin and the Flack parameter converged to 0.49(3). On account of the poor crystal quality, the hydrogen atoms of the two hydroxide ligands could not be located. CCDC-703000 contains the supplementary crystallographic data for this paper. These data can be obtained free of charge from The Cambridge Crystallographic Data Centre via [www.ccdc.cam.ac.uk/data\\_request/cif](http://www.ccdc.cam.ac.uk/data_request/cif).

## Acknowledgements

We thank the CNRS and MNEsR for financial support and Bertrand Revel (Centre Commun de Mesures RMN, USTL) for his assistance with NMR spectroscopy. Nord/Pas de Calais Region, Europe (FEDER), CNRS, French Ministry of Science, USTL, and ENSCL are thanked for funding the Bruker 18.8 T spectrometer. The Deutsche Forschungsgemeinschaft is kindly acknowledged for partial funding of this project in the framework of the Advanced Materials priority program (AM<sup>2</sup>-net). Prof. Dr. R. Boese and D. Bläser are thanked for measurement of the X-ray diffraction data.

[1] J. Guzman, B. C. Gates, *Dalton Trans.* **2003**, 3303–3318.

- [2] a) F. J. Feher, T. A. Budzichowski, *Polyhedron* **1995**, *14*, 3239–3253; b) R. Murugavel, A. Voigt, M. Ganapati Walawalkar, H. W. Roesky, *Chem. Rev.* **1996**, *96*, 2205–2236; c) R. Duchateau, *Chem. Rev.* **2002**, *102*, 3525–3542.
- [3] a) L. Bourget-Merle, M. F. Lappert, J. R. Severn, *Chem. Rev.* **2002**, *102*, 3031–3066; b) C. Floriani, *Chem. Eur. J.* **1999**, *5*, 19–23; c) L. Turculet, T. D. Tilley, *Organometallics* **2004**, *23*, 1542–1553; d) C. Janiak, H. Schumann, *Adv. Organomet. Chem.* **1991**, *33*, 291–393.
- [4] a) S. Harder, F. Feil, K. Knoll, *Angew. Chem.* **2001**, *113*, 4391; *Angew. Chem. Int. Ed.* **2001**, *40*, 4261; b) M. H. Chisholm, J. Gallucci, K. Phomphrai, *Chem. Commun.* **2003**, 48; c) Z. Zhong, S. Schneiderbauer, P. J. Dijkstra, M. Westerhausen, J. Feijen, *Polym. Bull.* **2003**, *51*, 175; d) M. R. Crimmin, I. J. Casely, M. S. Hill, *J. Am. Chem. Soc.* **2005**, *127*, 2042; e) F. Buch, J. Brettar, S. Harder, *Angew. Chem.* **2006**, *118*, 2807; *Angew. Chem. Int. Ed.* **2006**, *45*, 2741; f) M. R. Crimmin, A. G. Barrett, M. S. Hill, P. A. Procopiou, *Org. Lett.* **2007**, *9*, 331; g) S. Datta, P. W. Roesky, S. Blechert, *Organometallics* **2007**, *26*, 4392; h) F. Buch, S. Harder, *Organometallics* **2007**, *26*, 5132; i) A. G. Barrett, M. R. Crimmin, M. S. Hill, P. B. Hitchcock, G. Kociok-Köhn, P. A. Procopiou, *Inorg. Chem.* **2008**, *47*, 7366–7376; j) F. Buch, S. Harder, *Z. Naturforsch. B* **2008**, *62*, 169–177.
- [5] W. Schlenk, W. Schlenk, Jr., *Ber. Dtsch. Chem. Ges.* **1929**, *62*, 920–924.
- [6] S. Harder, F. Feil, A. Weeber, *Organometallics* **2001**, *20*, 1044–1046.
- [7] M. Westerhausen, W. Schwarz, *Z. Anorg. Allg. Chem.* **1991**, *604*, 127.
- [8] For an rare example of immobilization of an alkaline earth metal amide on mesoporous silica, see: a) C. Zapilko, R. Anwender, *Stud. Surf. Sci. Catal.* **2005**, *158*, 461–468. For selected examples of grafting of transition-metal benzyl complexes, see: b) D. G. H. Ballard, E. Jones, R. J. Wyatt, R. T. Murray, P. A. Robinson, *Polymer* **1974**, *15*, 169–174; c) N. G. Maksimov, G. A. Nesterov, V. A. Zakharov, P. V. Stchastnev, V. F. Anufrienko, Y. I. Yermakov, *J. Mol. Catal.* **1978**, *4*, 167–179; d) S. Nemana, B. C. Gates, *Langmuir* **2006**, *22*, 8214–8220; for selected examples of grafting of transition-metal amido complexes, see: e) Q. Zhuang, K. Tanaka, M. Ichikawa, *J. Chem. Soc. Chem. Commun.* **1990**, 1477–1478; f) R. Anwender, R. Roesky, *J. Chem. Soc. Dalton Trans.* **1997**, 137–138; g) A. O. Bouh, G. L. Rice, S. L. Scott, *J. Am. Chem. Soc.* **1999**, *121*, 7201–7210.
- [9] a) J. M. Thomas, R. Raja, D. W. Lewis, *Angew. Chem.* **2005**, *117*, 6614–6641; *Angew. Chem. Int. Ed.* **2005**, *44*, 6456–6482; b) C. Copéret, M. Chabanas, R. Petroff Saint-Arroman, J.-M. Basset, *Angew. Chem.* **2003**, *115*, 164–191; *Angew. Chem. Int. Ed.* **2003**, *42*, 156–181.
- [10] L. T. Zhuravlev, *Langmuir* **1987**, *3*, 316–318.
- [11] a) E. Le Roux, M. Chabanas, A. Baudouin, A. de Mallmann, C. Copéret, E. A. Quadrelli, J. Thivolle-Cazat, J.-M. Basset, W. Lukens, A. Lesage, L. Emsley, G. J. Sunley, *J. Am. Chem. Soc.* **2004**, *126*, 13391–13399; b) R. M. Gauvin, A. Mortreux, *Chem. Commun.* **2005**, 1146–1148.
- [12] See the Supporting Information.
- [13] I. Schnell, S. P. Brown, H. Y. Low, H. Ishida, H. W. Spiess, *J. Am. Chem. Soc.* **1998**, *120*, 11784–11795.
- [14] R. M. Gauvin, L. Delevoye, R. Ali Hassan, J. Keldenich, A. Mortreux, *Inorg. Chem.* **2007**, *46*, 1062–1070.
- [15] a) N. R. E. N. Impens, P. van der Voort, E. F. Vansant, *Microporous Mesoporous Mater.* **1999**, *28*, 217–232; b) W. Hertl, M. L. Hair, *J. Phys. Chem.* **1971**, *75*, 2181–2185; c) D. W. Sindorf, G. E. Maciel, *J. Phys. Chem.* **1982**, *86*, 5208–5219.
- [16] The  $\text{CaN}(\text{SiMe}_3)_2$  functionality has been shown to react with a large excess of  $\text{NH}_3$  to give a  $\text{CaNH}_2$  functionality: C. Ruspic, S. Harder, *Inorg. Chem.* **2007**, *46*, 10426–10433. The absence of ammonialysis during the synthesis of  $\text{SiO}_2\text{-2}$  may be due to the much lower concentration of  $\text{NH}_3$  formed in situ.
- [17] M. Westerhausen, *Inorg. Chem.* **1991**, *30*, 96–101.
- [18] a) For use of  $(t\text{BuO})_3\text{SiOH}$  as model for silica, see: A. Fischbach, M. G. Klimpel, M. Widenmeyer, E. Herdtweck, W. Scherer, R. Anwender, *Angew. Chem.* **2004**, *116*, 2284–2289; *Angew. Chem. Int.*

- Ed.* **2004**, *43*, 2234–2239; b) For its synthesis, see: J. Beckmann, *Appl. Organomet. Chem.* **2003**, *17*, 52–62.
- [19] C. Ruspic, S. Nembenna, A. Hofmeister, J. Magull, S. Harder, H. W. Roesky, *J. Am. Chem. Soc.* **2006**, *128*, 15000–15004.
- [20] W. Teng, M. Guino-o, J. Hitzbleck, U. Englich, K. Ruhlandt-Senge, *Inorg. Chem.* **2006**, *45*, 9531–9539.
- [21] a) V.-C. Arunasalam, I. Baxter, S. R. Drake, M. B. Hursthouse, K. M. Abdul Malik, D. J. Otway, *Inorg. Chem.* **1995**, *34*, 5295–5306; b) J. Utko, S. Przybylak, L. B. Jerzykiewicz, S. Szafert, P. Sobota, *Chem. Eur. J.* **2003**, *9*, 181–190.
- [22] V. Lorenz, S. Blaurock, F. T. Edelmann, *Z. Anorg. Allg. Chem.* **2008**, *634*, 441.
- [23] F. Feil, S. Harder, *Macromolecules* **2003**, *36*, 3446–3448.
- [24] D. F.-J. Piesik, K. Häbe, S. Harder, *Eur. J. Inorg. Chem.* **2007**, 5652–5661.
- [25] M. Ernst, *J. Magn. Reson.* **2003**, *162*, 1–34.
- [26] S. Hong, S. Tian, M. V. Metz, T. J. Marks, *J. Am. Chem. Soc.* **2003**, *125*, 14768.
- [27] G. M. Sheldrick, SHELXS-97, Program for Crystal Structure Solution, **1997**, Universität Göttingen, Germany.
- [28] G. M. Sheldrick, SHELXL-97, Program for Crystal Structure Refinement, **1997**, Universität Göttingen, Germany.
- [29] A. L. Spek, PLATON, A Multipurpose Crystallographic Tool **2000**, Utrecht University, Utrecht, The Netherlands.

Received: December 1, 2008

Published online: March 13, 2009